[46] H. F. Taylor, W. E. Martin, D. B. Hall, and V. N. Smiley, "Fabrication of single crystal semiconductor optical waveguides by solid state diffusion," *Appl. Phys. Lett.*, vol. 21, p. 95, 1972.
[47] W. E. Martin, "Waveguide electrooptic modulation in II-IV compounds," *J. Appl. Phys.*, vol. 44, p. 3703, 1973.
[48] a) W. E. Martin, "Photoluminescence determination of Cd diffusion in ZnSe," *J. Appl. Phys.*, vol. 44, p. 5639, 1973.
b) ——, "Refractive index profile measurements of diffused optical waveguides," *Appl. Optics*, vol. 13, p. 2112, 1974.
[49] J. R. Carruthers, I. P. Kaminow, and L. W. Stulz, "Outdiffusion kinetics and optical waveguiding properties of outdiffused layers in lithium niobate and lithium tantalate," *Appl. Opt.*, vol. 13, p. 2333, 1974.
[50] a) N. F. Hartman, R. P. Kenan, P. R. Sievert, C. M. Verber, and V. E. Wood, "Characteristics of diffused waveguiding layers in $LiNbO_3$," presented at the Integrated Optics Meeting, New Orleans, 1974.
b) V. E. Wood, N. F. Hartman, and C. M. Verber, "Characteristics of diffused slab waveguides in $LiNbO_3$," *J. Appl. Phys.*, vol. 45, p. 1449, 1974.
[51] I. P. Kaminow, J. R. Carruthers, E. H. Turner, and L. W. Stulz, "Thin-film $LiNbO_3$ electrooptic light modulator," *Appl. Phys. Lett.*, vol. 22, p. 540, 1973.
[52] a) R. V. Schmidt, I. P. Kaminow, and J. R. Carruthers, "Acoustooptic diffraction of guided optical waves in $LiNbO_3$," *Appl. Phys. Lett.*, vol. 23, p. 417, 1973.
b) J. Noda, N. Uchida, and T. Saku, "Electrooptic diffraction modulator using outdiffused waveguiding layer in $LiNbO_3$," *Appl. Phys. Lett.*, vol. 25, p. 131, 1974.
[53] a) J. M. Hammer and W. Phillips, "Low-loss single-mode optical waveguides and efficient high-speed modulators at $LiNb_xTa_{1-x}O_3$ on $LiTaO_3$," *Appl. Phys. Lett.*, vol. 24, p. 545, 1974.
b) R. V. Schmidt and I. P. Kaminow, "Metal-diffused optical waveguides on $LiNnO_3$," *Appl. Phys. Lett.*, vol. 25, p. 458, 1974.
c) R. D. Standley and V. Ramaswamy, "Nb-diffused $LiTaO_3$ optical waveguides: planar and embedded strip guides," *Appl. Phys. Lett.*, vol. 25, p. 711, 1974.
d) J. Noda, T. Saku, and N. Uchida, "Fabrication of optical waveguiding layer in $LiTaO_3$ by Cu diffusion," *Appl. Phys. Lett.*, vol. 25, p. 308, 1974.
e) R. V. Schmidt and I. P. Kaminow, "Acoustooptic Bragg deflection in $LiNbO_3$ Ti-diffused waveguides," *IEEE J. Quantum Electron.* (Corresp.), vol. QE-11, pp. 57–59, Jan. 1975.
[54] F. Zernike, private communication.
[55] S. E. Miller, "Coupled wave theory and waveguide applications," *Bell Syst. Tech. J.*, vol. 33, p. 661, 1954.
[56] S. Kurazono, K. Iwasaki, and N. Kumagi, "A new optical modulator consisting of coupled optical waveguides," *J. Inst. Electron. Commun. Eng. Jap.*, vol. 55C, p. 103, 1972.
[57] S. Wang, M. Shah, and J. D. Crow, "Studies of the use of gyrostropil and anisotropic materials for mode conversion in thin-film optical-waveguide applications," *J. Appl. Phys.*, vol. 43, p. 1961, 1972.
[58] L. Kuhn, P. F. Heidrich, and E. G. Lean, "Optical guided wave mode conversion by an acoustic surface wave," *Appl. Phys. Lett.*, vol. 19, p. 428, 1971.
[59] I. P. Kaminow and H. Kogelnik, unpublished.
[60] a) W. S. C. Chang, "Acoustooptical deflections in thin films," *IEEE J. Quantum Electron.* (Corresp.), vol. QE-7, pp. 167–170, Apr. 1971.
b) ——, "Periodic structures and their application in integrated optics," *IEEE Trans. Microwave Theory Tech.* (*1973 Symposium Issue*), vol. MTT-21, pp. 775–785, Dec. 1973.
[61] a) F. R. Gfeller and C. W. Pitt, "Collinear acoustooptic deflection in thin films," *Electron. Lett.*, vol. 8, p. 549, 1972.
b) F. R. Gfeller, "Acoustooptic scanner," presented at the Integrated Optics Meeting, New Orleans, 1974.
[62] a) L. Figueroa and I. P. Kaminow, unpublished.
b) D. Marcuse, "Light scattering from periodic refractive index fluctuations in asymmetric slab waveguides," *IEEE J. Quantum Electron.*, to be published.
[63] I. P. Kaminow, W. Mammel, and H. P. Weber, "Metal-clad optical waveguides: Analytical and experimental study," *Appl. Opt.*, vol. 13, p. 396, 1974.
[64] I. P. Kaminow, unpublished.
[65] W. R. Klein and B. D. Cook, "Unified approach to ultrasonic light diffraction," *IEEE Trans. Sonics Ultrason.*, vol. SU-14, pp. 123–134, July 1967.
[66] a) Y. Ohmachi, "Acoustooptical light diffraction in thin films," *J. Appl. Phys.*, vol. 44, p. 3928, 1973.
b) Y. Ohmachi, "Acoustooptic TE_0–TM_0 mode conversion in a thin-film of amorphous tellurium dioxide," *Electron. Lett.*, vol. 9, p. 539, 1973.
[67] H. Engan, "Excitation of elastic surface wave eaves by spatial harmonics of interdigital transducers," *IEEE Trans. Electron Devices*, vol. ED-16, pp. 1014–1017, Dec. 1969.
[68] L. Kuhn, M. L. Dakss, P. F. Heidrich, and B. A. Scott, "Deflection of an optical guided wave by a surface acoustic wave," *Appl. Phys. Lett.*, vol. 6, p. 265, 1970.
[69] R. V. Schmidt, unpublished.
[70] M. A. R. P. deBarros and M. G. F. Wilson, "High speed electrooptic diffraction modulator for baseband operation," *Proc. Inst. Elec. Eng.* (London), vol. 119, p. 807, 1972.
[71] S. Wright and M. G. F. Wilson, "New form of electrooptic deflector," *Electron. Lett.*, vol. 9, p. 169, 1973.
[72] T. L. Paoli and J. E. Ripper, "Direct modulation of semiconductor lasers," *Proc. IEEE* (*Special Issue on Optical Communication*), vol. 58, pp. 1457–1465, Oct. 1970.
[73] M. Chown, A. R. Goodwin, D. F. Lovelace, G. H. B. Thompson, and P. R. Selway, "Direct modulation of double-heterostructure lasers at rates up to 1 Gbit/s," *Electron. Lett.*, vol. 9, p. 34, 1973.

Nonreciprocal Magnetooptic Waveguides

JOHN WARNER

Abstract—**The longitudinal magnetooptic effect can be used in a unique way to mix TE and TM modes of a planar dielectric waveguide where the strength of mixing is dependent upon propagation direction (forwards or reverse). A detailed study of Faraday effect circulators in optical dielectric waveguides is presented and accurate design data for a practical version are offered. At this writing, experimental confirmation has been hampered by lack of success in optically contacting two dissimilar materials.**

Manuscript received March 21, 1974; revised July 8, 1974. This work was supported in part by the Advanced Research Projects Agency, ARPA Order 2327 and is published by permission of Her Brittanic Majesty's Stationary Office.

The author was with the U. S. Naval Research Laboratory, Washington, D. C. He is now with the Royal Radar Establishment, Malvern, Worcs., England.

I. INTRODUCTION

THE development of integrated optics is still at the stage where experiments on components for detection, modulation, and switching are being reported. We would like to add to these reports with our detailed study of how

materials exhibiting the Faraday effect might be incorporated into a planar optical waveguide to produce a miniature optical circulator or isolator. The Faraday effect produces a rotation of the plane of polarization of linearly polarized light as it passes through a bulk magnetooptic medium. The rotation is right handed (say) for light traveling with the magnetic field and left handed (say) for light against the field. This nonreciprocal nature has been exploited at microwave (waveguide modes) and optical (bulk-wavemodes) frequencies to make one-way transmission devices or isolators [1]. The situation is complicated in planar optical waveguides because circularly polarized propagation modes (which are used to explain the optical rotation of linearly polarized light) do not normally propagate in planar waveguides [2].

In this paper we first of all summarize the essential features of a bulk-wave optical isolator, indicating what refinements over the basic configuration are required before dielectric waveguide analogues can be conceived. We then outline our path towards a practical design of dielectric waveguide isolator. This particular design has been given a thorough theoretical analysis, as outlined in Section III, and a practical version based on magnetic garnet films has been the subject of our experimental program. We give design data in Section IV and at the end of the report give a summary of our achievements to date.

II. BASIC DESIGN CONSIDERATIONS

A. Bulk-Wave Optical Isolators

Fig. 1 illustrates the longitudinal magnetooptic or Faraday effect which is exploited in the design of optical isolators and circulators. An optical beam is sent through a magnetooptic crystal parallel to an applied magnetic field. Linearly polarized light traveling with the field will find its polarization direction rotated as a right-hand screw (say), whereas light traveling against the field is rotated in the opposite sense (a left-hand screw in our example). This rotation is similar to that experienced in optically active crystals with one important difference; the magnetic medium experiences right- and left-hand rotation, whereas the sense of rotation in an optically active medium is not changed by reversing the propagation direction. If the path length in the magnetooptic crystal is such that a 45° rotation is achieved, we are able by the simple addition of two linear polarizers at suitable azimuth orientations, to devise "one-way" transmission characteristics which constitute an optical isolator. Fig. 2 shows that the polarizers are set at 45° to each other. Vertically polarized light, traveling with the applied magnetic field, passes through the input polarizer, and is then rotated with a right-hand screw motion to 45° azimuth where it is correctly oriented to pass through the second polarizer. If this 45° polarized light is sent back against the field direction it would be rotated with a left-hand screw motion to a 90° azimuth to be blocked by the polarizer at 0° azimuth. In this way a combination of two polarizers set at 45° to each other and a 45° Faraday rotator will act as an optical isolator, permitting transmission in one direction only.

Waveguide modes in planar dielectric waveguides have their electric vectors vibrating in orthogonal planes. The simple bulk isolator described earlier will *not* therefore carry over to a waveguide version, because the input and output polarizations are at 45° not 0 or 90°. A second active element must be included so that the output polarization is brought back to 0° azimuth as illustrated in Fig. 3. A 45° optically active rotator with a left-hand sense of rotation is inserted between the magnetic rotator and the second polarizer. This brings light vibrating at 45° azimuth to the vertical for *both directions of propagation*. Thus we can see intuitively that we need *two* active media to make an optical waveguide isolator. It is also implicit in these bulk wave isolators that the vertical and horizontal polarizations travel in-phase and the observed rotation of the direction of vibration is a consequence of the coupling between these polarizations. This phase-

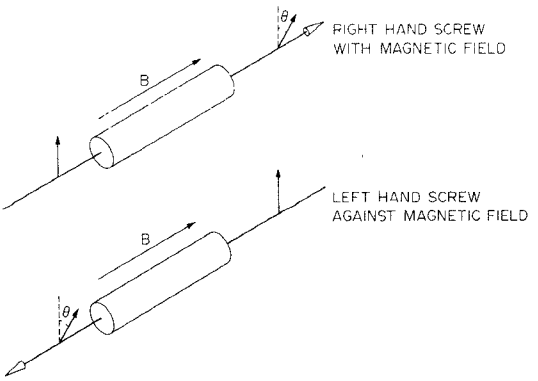

Fig. 1. Faraday effect.

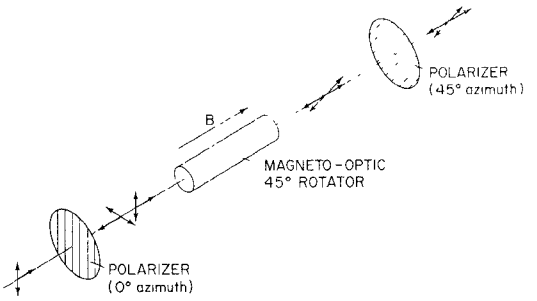

Fig. 2. Basic isolator.

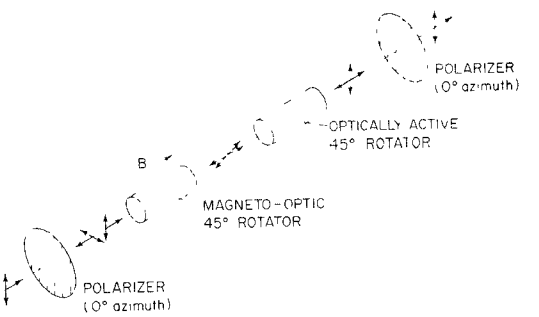

Fig. 3. Isolator with parallel polarizers.

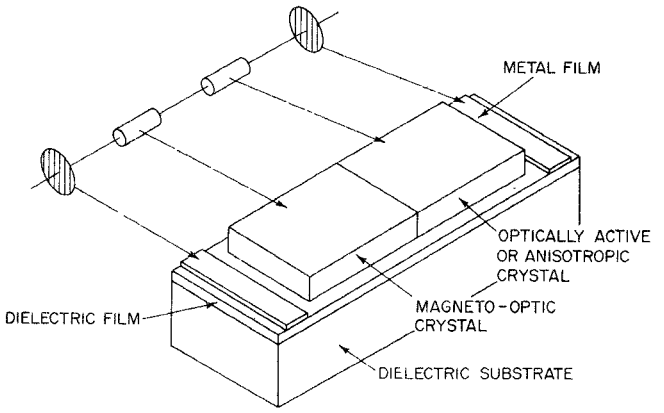

Fig. 4. Waveguide isolator after Wang [3].

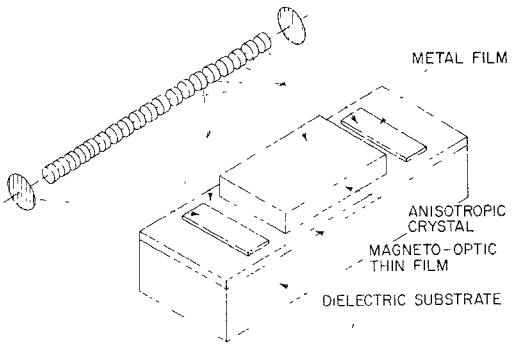

Fig. 5. Improved waveguide isolator.

matching requirement carries over to the optical waveguide cases where the TE and TM modes must travel in phase.

B. Planar Dielectric Waveguide Isolators

A waveguide version of Fig. 3 has been proposed by Wang *et al.* [3] in which magnetooptic and optically active (or anisotropic) crystals are placed in tandem on top of a dielectric waveguide as shown in Fig. 4. The waveguide mode fields penetrate into these regions but decay exponentially as they do so. It is possible to replace the optically active crystal with an anisotropic one in optical waveguide cases because TM modes have a component of electric field along the propagation direction and an anisotropic crystal can be oriented to provide a coupling between this field component and the electric field of a TE mode.

The magnetooptic effect only provides a weak coupling between TE and TM fields and since in Fig. 4 there is only a small penetration of the mode field into the top layers the amount of mode conversion attainable would be quite small. This in turn calls for a requirement of accurate phase matching between the TE and TM modes over long distances (on the order of 10–20 mm). Mode degeneracy cannot be achieved in a dielectric waveguide made with optically isotropic materials (see Section III-B) and so the waveguide structure supporting the magneto-optic and anisotropic crystals would itself have to be made from anisotropic materials.

A much better basic design is achieved if the essential materials (i.e., the magnetooptic and anisotropic layers) are regrouped as shown in Fig. 5. In this configuration the magnetooptic film forms the high index guiding layer and consequently is situated where the waveguide modes are most strongly located. Also the anisotropic layer, which is placed as a superstrate over the magnetic film, performs the double role of providing mode conversion complementary to that of the magnetic film, and allowing the possibility of degenerate-mode propagation or phase matching. Fig. 5 illustrates that the bulk-wave analogue of this preferred geometry is one in which the anisotropic and optically active 45° rotators are sliced up into small sections which are then interleaved.

It is the basic design of Fig. 5 which was chosen by us as the best candidate for experimental study. A survey of technically proven materials reveals that the best choice for experimentation comprises a magnetic garnet film grown on gadolinium gallium garnet with $LiIO_3$ acting as the anisotropic superstrate. Detailed design data for this system, based on the theory outlined in the next section, are presented in Section IV.

III. THEORETICAL ANALYSIS OF OPTICAL WAVEGUIDE ISOLATOR

We now outline our theoretical analysis of an optical waveguide isolator/gyrator formed by a magnetooptic film sandwiched between an isotropic and an anisotropic layer as shown in Fig. 5. The mode-conversion analysis follows the ray-optical approach of Kogelnik *et al.* [4] which includes the Goos–Haenchen effects. That analysis is followed by a brief summary of how the anisotropic crystal which provides mode conversion complementary to the magnetic film also provides for degenerate-mode propagation.

A. Derivation of Coupled Mode Equations

In Fig. 6 we depict the zigzag ray path of a TE wave in the waveguide. Mode conversion due to the magnetic film will occur along the paths *BC* and *DE* and that due to the anisotropic layer will occur upon reflection at *CD*. In each case the mode conversion may be described in

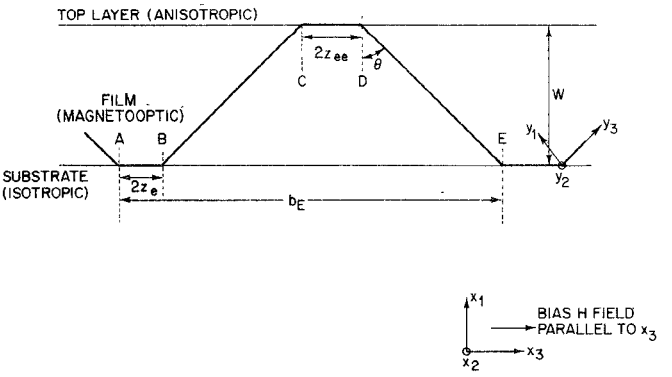

Fig. 6. Zigzag path of TE wave in a planar waveguide.

terms of a coupling matrix where the off-diagonal terms represent the mode conversion coefficients. In general we write

$$\begin{bmatrix} \mathrm{TE}_{\mathrm{out}} \\ \\ \mathrm{TM}_{\mathrm{out}} \end{bmatrix} = \begin{bmatrix} R_{11} & R_{12} \\ \\ R_{21} & R_{22} \end{bmatrix} \begin{bmatrix} \mathrm{TE}_{\mathrm{in}} \\ \\ \mathrm{TM}_{\mathrm{in}} \end{bmatrix}. \tag{1}$$

There is no mode conversion at the substrate boundary because the substrate is optically isotropic. The mode coupling matrix for reflection at the substrate boundary therefore has zero off-diagonal terms and is given by

$$[R_S] = \begin{bmatrix} \exp(2i\phi_e) & 0 \\ \\ 0 & \exp(2i\phi_m) \end{bmatrix} \tag{2}$$

where ϕ_e and ϕ_m are the Goos–Haenchen phase shifts associated with the total internal reflection.

The anisotropic top layer is oriented in such a way that the permittivity tensor has the element ϵ_{23} nonzero when expressed in the coordinate system (x_i) shown in Fig. 6. The mode coupling matrix for this reflection is [3]

$$[R_T] = \begin{bmatrix} r\exp(2i\phi_{ee}) & s\exp(2i\phi_{em}) \\ \\ -s\exp(2i\phi_{em}) & r\exp(2i\phi_{mm}) \end{bmatrix}. \tag{3}$$

r,s and ϕ's have been related to material parameters by Wang *et al.* [3] and, for convenience, these relations are tabulated in Appendix I.

The mode coupling matrix applicable to a single passage through the magnetooptic film (either B to C or D to E) is derived in Appendix II and is given by

$$[R_F] = \exp(i\Delta) \begin{bmatrix} \cos\psi & -\sin\psi \\ \\ \sin\psi & \cos\psi \end{bmatrix} \tag{4}$$

where

$$\Delta = -\frac{k_0 n_f W}{\cos\theta} \quad \text{and} \quad \psi = -\frac{k_0 G W \tan\theta}{2n_f}.$$

In adopting the analytical approach of Kogelnik *et al.* [4] we use the matrices given by (2)–(4) to write down the TE and TM fields at each end of a complete zigzag cycle. These are then related by a Taylor's series expansion to the field derivatives and, after some algebra, a pair of coupled differential equations emerge as

$$\frac{dA_E}{dz} + i(\beta - \beta_E)A_E = iKA_M$$

$$\frac{dA_M}{dz} + i(\beta - \beta_M)A_M = iKA_E. \tag{5}$$

A_E and A_M are the normalized TE and TM field amplitudes. β_E and β_M are the propagation constants of the TE and TM modes, and K is a coupling coefficient between the modes given by

$$K = \frac{s\cos^2\psi + r\sin 2\psi\cos(\phi_{ee} - \phi_{mm})}{(b_e b_m)^{1/2}}. \tag{6}$$

b_e and b_m are the round trip bounce lengths illustrated in Fig. 6.

Equation (6) shows us how nonreciprocal mode conversion effects arise. If the propagation direction is reversed with respect to the magnetization direction, G and hence ψ will change sign. If we take care to match the magnitude of the two terms in the numerator of (6), then nonreciprocal mode conversion will be achieved; K being nonzero in the forward direction (say) but zero in the reverse direction. The interaction length for complete mode conversion may be found from the solutions to (5). If all the light is in the TE wave at $z = 0$ then [5]

$$A_M(z) = A_E(0)\sin[Kz(1+Q^2)^{1/2}]/[1+Q^2]^{1/2} \tag{7}$$

where the phase mismatch factor $Q = (\beta_E - \beta_M)/2K$.

The maximum converted light intensity falls from 100 to 50 percent for $Q = 0.80$. Such a value of Q allows one to estimate a practical tolerance on the phase matching between TE and TM modes. This point is considered further in Section IV.

We see from (7) that complete conversion will occur in a distance l_{opt} for which $l_{\mathrm{opt}}K = \pi/2$. For the material parameters given in Section IV, we find that $l_{\mathrm{opt}} \sim 2$ mm.

B. Phase Matching for Degenerate Modes

It is evident from (7) that the TE and TM modes between which we have arranged nonreciprocal coupling must propagate degenerately in order for complete TE to TM (and vice versa) conversion to take place. The diagonal terms of the mode-conversion matrices given by (2)–(4) can be used to obtain expressions for the TE and TM propagation constants β_E and β_M. In order for a proper waveguide mode to exist, the phase delay of a zigzag wave traversing the path A–B–C–D–E in the film (Fig. 6 refers) must be the same as that of an evanescent wave traveling in the substrate from A to E. After some algebra, this requirement reduces mathematically to the following equations:

$$W_{\mathrm{TE}} = \frac{\Delta}{2\pi}\left\{\left[m\pi + \tan^{-1}\left(\frac{(n_g^2 - n_y^2)}{(n_f^2 - n_g^2)}\right)^{1/2} + \tan^{-1}\left(\frac{(n_g^2 - n_s^2)}{(n_f^2 - n_g^2)}\right)^{1/2} \Big/ (n_f^2 - n_g^2)\right]\right\} \tag{8}$$

$$W_{\mathrm{TM}} = \frac{\Delta}{2\pi}\left(\left\{m\pi + \tan^{-1}\left[\left(\frac{n_f^2}{n_x n_z}\right)^2 \frac{(n_g^2 - n_x^2)}{(n_f^2 - n_g^2)}\right]^{1/2} + \tan^{-1}\left[\left(\frac{n_f}{n_s}\right)^4 \frac{(n_g^2 - n_s^2)}{(n_f^2 - n_g^2)}\right]^{1/2} \Big/ (n_f^2 - n_g^2)\right\}\right) \tag{9}$$

where n_g is the effective guide index β/k_0 and n_x, n_y, n_z are the refractive indices of the anisotropic top layer. Degen-

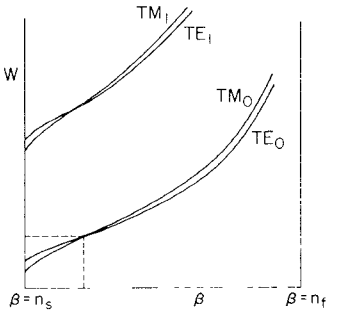

Fig. 7. Mode dispersion diagram showing degeneracy.

erate modes are achieved when $W_{TE} = W_{TM}$ for a special value of n_g. Let us examine how this might be achieved if the anisotropic crystal is a negative uniaxial crystal with its optic axis in the film plane, roughly perpendicular to the propagation direction. For this configuration $n_x = n_z = n_0$, the ordinary refractive index, and $n_y = n_e$, the extraordinary refractive index. Now $n_f > n_s$ for any waveguide and this gives a tendency for W_{TM} to be greater than W_{TM} for any value of n_g due to the factor $(n_f/n_s)^4$ in the second arctan term in (9). Since $n_e < n_0$ in a negative uniaxial crystal we may find a value of n_g close to n_0 for which $(n_f^2/n_0^2)^2(n_g^2 - n_0^2) < (n_g^2 - n_e^2)$ by just the amount to counter the factor $(n_f/n_s)^4$ yielding the result $W_{TE} = W_{TM}$. This situation is illustrated diagrammatically in Fig. 7.

IV. DESIGN DATA FOR $LiIO_3$–YIG–GGG WAVEGUIDE STRUCTURE

In order to attempt an experimental demonstration of a waveguide isolator in a short time scale we must select our materials from those whose growth technology has been well developed for other reasons. Magnetic garnet films, grown epitaxially on to gadolinium gallium garnet (GGG) have received a lot of attention as magnetic bubble-domain memory media. These films are immediately suitable as optical waveguides, the magnetic films having a higher refractive index than GGG. The only change required for our purpose is to move the magnetization axis from normal to the film plane to in the film plane. This is achieved by altering the film composition slightly to change the lattice parameter mismatch between the film and substrate. The films supplied to us by R. Henry of Rockwell International (Anaheim) have the composition $(LaY)_3Ga_{0.33}Fe_{4.67}O_{12}$ and are grown by liquid phase epitaxy on to ⟨111⟩ oriented GGG. The transmission spectrum of the magnetic garnets demands the use of a 1.06 μm or, for even smaller absorption, a 1.152-μm laser beam. We use a CW HeNe laser operation at 1.152 μm in our experiments. Having settled on materials for the film and substrate, the anisotropic top layer has to be chosen. The constraints are that the refractive indices should lie within a range (which proves to be small) over which mode degeneracy could be achieved. This phase-matching requirement also demands that the material shall be either a negative uniaxial crystal, or a biaxial crystal with a large optic angle. It would appear that

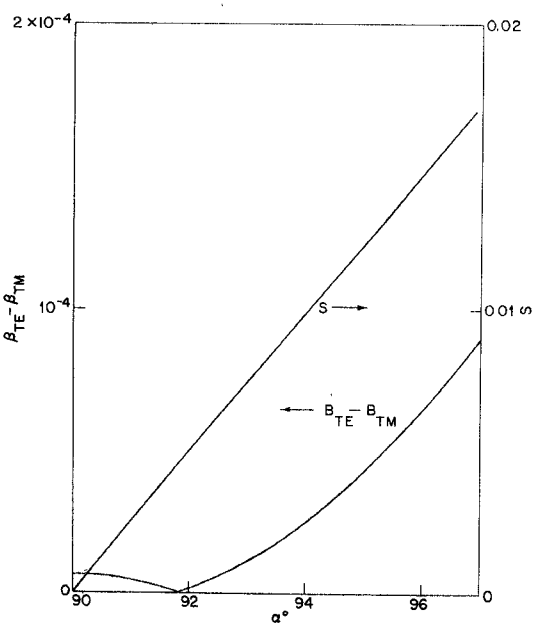

Fig. 8. Variation of β_{TE}–β_{TM} and S with crystal orientation.

lithium iodate ($LiIO_3$) is about the only suitable material with a developed growth technology.

Final design data may be obtained from the theory outlined in Section III, once the refractive indices of the materials are known. We know from Section III-B that the optic axis of $LiIO_3$ should be set roughly perpendicular to the propagation direction in order to most readily achieve degenerate modes.

We first assume that the optic axis is indeed at 90° to the propagation direction and use (8) and (9) to calculate the thickness for which the TE and TM modes are degenerate. In bulk YIG the Faraday effect produces about 280°/cm optical rotation at 1.152 μm [6]. This corresponds to $G = 3.4 \times 10^{-4}$ and we therefore have all the information needed to compute the magnetooptic mode coupling ψ given by (4). We next use (6) to find the anisotropic mode coupling term s that yields zero mode conversion. s in turn is related to the angle ψ that the optic axis makes with the propagation direction via the equations given in Appendix I. It turns out that $\alpha \simeq 88°$ for our case and furthermore the phase matching is insensitive to α, whereas the coupling term s is roughly proportional to α as shown in Fig. 8. This fact gives us the experimentally convenient feature that α can be readily altered by suitably tilting the waveguide assembly, and doing this will "tune-in" the correct value of s without materially altering the mode-degeneracy condition.

The required design data are summarized in Table I. In this table the refractive indices of the garnet film and substrate were measured from a knowledge of prism coupling angles [7] and those for $LiIO_3$ top layer were taken from the literature [8]. All other data emerge from calculations based on the theory given in Section III. For example, the tolerance figure on the design film thickness of 1.935 μm is computed from the allowable phase mismatch introduced by letting the maximum converted light

TABLE I
DESIGN DATA FOR $LiIO_3$–YIG–GGG WAVEGUIDE ISOLATOR FOR 1.152-μM OPERATION

Substrate	Top Layer
Single crystal $Gd_3 Ga_5 O_{12}$	Single crystal $LiIO_3$ (optically contacted)
Film grown on <111> surface	$n_0 = 1.858$, $n_e = 1.716$
$n_s = 1.945 \pm .001$	Optic axis about 88 degrees from z in (y - z) plane
Magneto Optic Film	Length for complete mode conversion $\simeq 2$mms
$(LaY)_3 Ga_{.33} Fe_{4.67} O_{12}$ grown by LPE	$\phi_{ee} - \phi_{mm} = 87.0° - 79.4° = 7.6°$
$n_f = 2.1783 \pm .0004$	Waveguide mode decay const into top layer
$W = 1.39 \pm .03$ μm	a) for TE mode 1.08 μm
$G = 3.4 \times 10^{-4}$ (≡ 280°/cm Faraday Rotation)	b) for TM mode 1.70 μm

intensity fall from 100 to 50 percent. It should be noted that a maximum of 50-percent mode conversion would still allow a good demonstration of nonreciprocal propagation because, in the reverse direction, we can still arrange for there to be no mode coupling.

V. EXPERIMENTS ON "ONE-WAY" MODE CONVERSION

Our experimental program to study nonreciprocal effects in optical waveguides is centered on a GGG–YIG–$LiIO_3$ waveguide of appropriate dimensions and a pair of rutile right-angle prisms acting as input/output couplers as depicted in Fig. 9. We apply a magnetic bias field parallel to the propagation direction, couple into the TE mode, and look at the amount of TM light that emerges. Nonreciprocal effects will be evident if the amount of mode conversion changes when the bias field is reduced. The $LiIO_3$ orientation could be altered to minimize the smaller amount of conversion. An index-matching liquid under the rutile prisms minimizes mismatch reflections between the prism/YIG/GGG and $LiIO_3$–YIG–GGG regions.

Unfortunately, our experiments have not been successful in demonstrating nonreciprocal effects. We attribute this to our failure to get the $LiIO_3$ and garnet films in close enough contact. We have seen small amounts of mode conversion [9] insensitive to bias field reversal, but the TE and TM modes are not degenerate, indicating that the anistropy of the $LiIO_3$ is not playing its part.

We have studied the mode dispersion curves for a four layer waveguide where we have introduced a thin gap of thickness t between the $LiIO_3$ and the garnet film. In Fig. 10 we plot TE and TM curves for several values of t. We see that the gap is a critical factor in the location of the degenerate mode point. What happens is that the waveguide mode field decays into the gap and consequently the $LiIO_3$ is quickly screened from the mode. It only takes $t = 0.1$ μm to remove any prospects of mode degeneracy. A gap of less than 0.1 μm infers a good optical contact. We could not optically contact our samples; a better optical finish will have to be obtained.

Alternatively, we could place a high-index liquid layer between the $LiIO_3$ and the garnet film. If the refractive

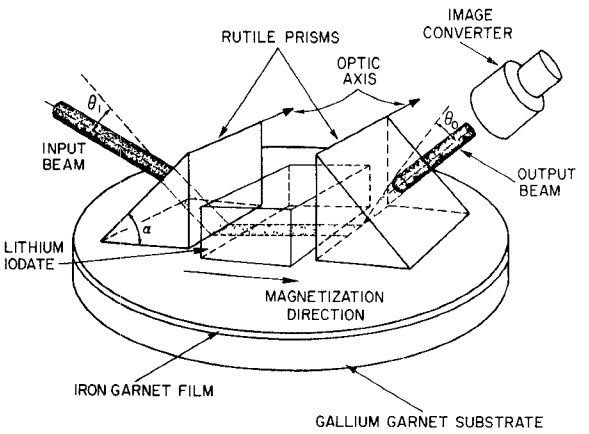

Fig. 9. Experimental arrangement.

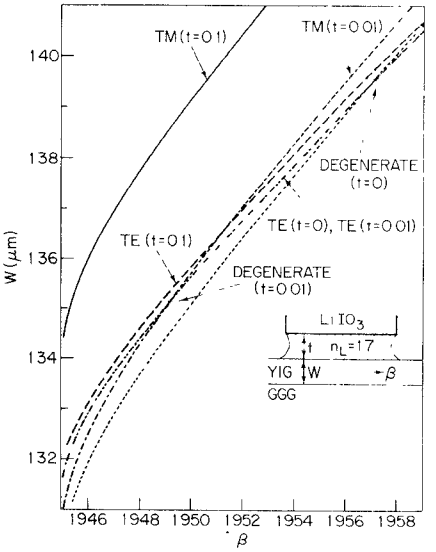

Fig. 10. Mode dispersion diagram showing effect of thin liquid layer on mode degeneracy.

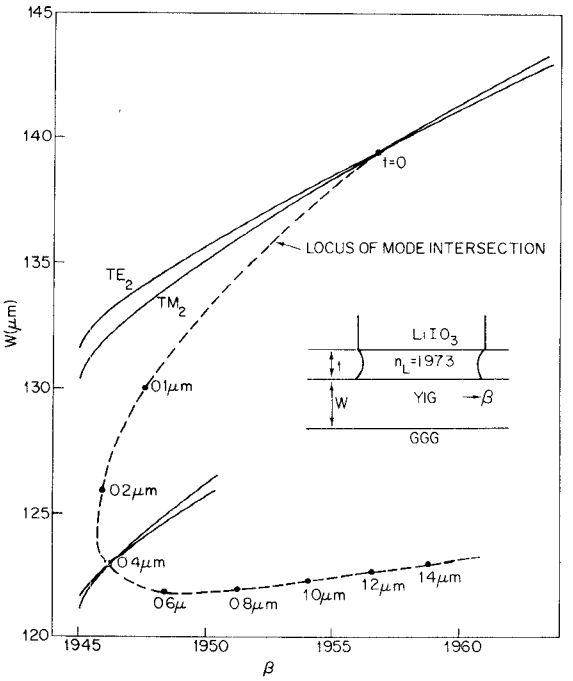

Fig. 11. Mode dispersion diagram showing locus of mode degeneracy with high index liquid layer.

index of this liquid were greater than the effective guide index of the waveguide modes of interest then we would get a sinusoidal field pattern in the liquid layer instead of an exponential decay and the $LiIO_3$ would continue to be effective. We have such a liquid at hand; it is a Cargille Laboratories index matching liquid from their EH series. Its refractive index for the soidum D line is 2.04, we measure $n = 1.973$ and $\alpha = 0.9$ cm^{-1} at 1.152 μm. Unfortunately, the material contains arsenic tribromide which reacts with the $LiIO_3$ and so we cannot use it. We have explored the location of the generate-mode operation points as a function of the thickness of a liquid layer of index 1.973. We see that the possibilities for degenerate modes persist to quite thick films as shown in Fig. 11. Furthermore, the phase-matching condition is insensitive to the exact liquid layer thickness if it is in the range of 0.5–1.0 μm.

VI. SUMMARY

We have identified the requirements for a magnetooptic isolator in an optical dielectric waveguide. The provision of a magnetooptic medium is necessary but not sufficient. We must also provide an anisotropic medium to give us the capability of achieving degenerate modes in the waveguide, and to provide a mode-coupling coefficient complementary to the magnetic one. A periodic structure like Tien's serpentine circuit [10] cannot be used to make up for a mode mismatch since any such structure destroys the unique symmetry of the longitudinal magnetooptic effect which produces nonreciprocal phenomena. We have carried out a detailed theoretical study of the problem and are confident that our design is the best choice based on currently available materials. We use a layered structure in which an iron garnet film is grown epitaxially on to GGG and a $LiIO_3$ crystal is optically contacted to the film to form a superstrate. We have been successful in getting all the materials to the required dimensions, etc., and have demonstrated our ability to measure critical parameters like film thickness to adequate accuracy.

So far we have failed to demonstrate nonreciprocal effects. We are confident that this is due to our inability to optically contact the $LiIO_3$ to the garnet film. The available samples had somewhat relaxed tolerances on optical flatness, etc. New samples, with better optical finish will become available and we look forward to better success in optically contacting these satisfactorily.

An alternative avenue for further research would be to explore the possibilities of nonisotropic magnetooptic materials in which the magnetic and anisotropic mode coupling would take place in the same film. At this writing, we have not begun to analyze such systems in any detail. A possible material class would be the orthoferrites. Study would be required to determine whether the phase-matching possibilities could lead to experimentally attractive situations like that found in the system described in this paper. We refer here to the happy situation illustrated in Fig. 8 where orientation adjustments change the mode coupling coefficient by large amounts, whereas the phase matching is hardly affected. Preliminary investigations suggest that this type of behavior does not normally occur in waveguides with anisotropic films.

APPENDIX I

MODE CONVERSION MATRIX FOR REFLECTION AT ANISOTROPIC DIELECTRIC BOUNDARY

Wang *et al.* [3] have derived expressions relating the reflection and mode conversion that takes place between TE and TM waves upon total internal reflection at a boundary between an isotropic medium of high refractive index and an optically unaxial medium whose optic axis lies in the boundary plane. For convenience, their expressions are copied out as follows:

$$\begin{bmatrix} \mathrm{TE}_{\mathrm{out}} \\ \mathrm{TM}_{\mathrm{out}} \end{bmatrix} = \begin{bmatrix} r_{ee} & -r_{em} \\ r_{em} & r_{mm} \end{bmatrix} \begin{bmatrix} \mathrm{TE}_{\mathrm{in}} \\ \mathrm{TM}_{\mathrm{in}} \end{bmatrix} \tag{A.1}$$

where

$$r_{ee} = \frac{1}{F}\left(\frac{G_1 J_2^*}{L_1} - \frac{G_2 J_1^*}{L_2}\right) \tag{A.2a}$$

$$r_{em} = \frac{2(p_1 - p_2) n_f \cos\theta}{F K_{23}} \tag{A.2b}$$

$$r_{mm} = \frac{1}{F}\left(\frac{G_1^* J_2}{L_1} - \frac{G_2^* J_1}{L_1}\right) \tag{A.2c}$$

and

$$F = \frac{G_1 J_2}{L_1} - \frac{G_2 J_1}{L_2} \tag{A.3a}$$

$$G_{1,2} = p_{1,2} K_{11} \cos\theta - i(n_g^2 - K_{11}) n_f \tag{A.3b}$$

$$J_{1,2} = n_f \cos\theta - i p_{1,2} \tag{A.3c}$$

$$L_{1,2} = n_g^2 K_{33} - K_{11} K_{33} - K_{11} p_{1,2}^2. \tag{A.3d}$$

In the preceding expressions p_1 and p_2 are the decay constants of the evanescent waves into the anisotropic layer, given by

$$p_{1,2}^2 = \frac{1}{2K_{11}} \{A + [B^2 - 4K_{11}K_{23}^2(n_g^2 - K_{11})]^{1/2}\} \tag{A.4a}$$

where

$$A = n_g^2(K_{11} + K_{33}) - K_{11}(K_{22} + K_{33}) \tag{A.4b}$$

$$B = n_g^2(K_{11} - K_{33}) - K_{11}(K_{22} - K_{33}) \tag{A.4c}$$

$$C = n_g^2(K_{11} + K_{33}) - K_{11}(K_{22} - K_{33}). \tag{A.4d}$$

n_g is the effective guide index β/k_0 and the K_{ij} are the permittivity tensor coefficients for the uniaxial layer. If the optic axis makes an angle of α with the propagation direction we find that

$$(K_{ij}) = \begin{bmatrix} n_0^2 & 0 & 0 \\ 0 & n_0^2\cos^2\alpha + n_e^2\sin^2\alpha & (n_e^2 - n_0^2)\cos\alpha\sin\alpha \\ 0 & (n_e^2 - n_0^2)\cos\alpha\sin\alpha & n_e^2\cos^2\alpha + n_0^2\sin^2\alpha \end{bmatrix}. \quad (A.5)$$

r_{ee}, r_{em}, r_{mm} are, in general, complex quantities. In Section III of this paper they are referred to in a modulus and phase angle form.

$$r_{ee} = r\exp(i\phi_{ee})$$
$$r_{mm} = r\exp(i\phi_{mm})$$
$$r_{em} = s\exp[i\tfrac{1}{2}(\phi_{ee} + \phi_{mm})]. \quad (A.6)$$

For a given configuration r, s, ϕ_{ee}, and ϕ_{mm} are readily obtained by numerical computation from (A.2).

APPENDIX II

MODE CONVERSION MATRIX FOR CUBIC MAGNETOOPTIC WAVEGUIDING FILM

The amount of TE to TM conversion (and vice versa) that takes place during a single traverse of the "zigzag" plane wave that makes up the waveguide mode may be described in terms of a matrix R where

$$\begin{bmatrix} \mathrm{TE}_{\mathrm{out}} \\ \mathrm{TM}_{\mathrm{out}} \end{bmatrix} = [R]\begin{bmatrix} \mathrm{TE}_{\mathrm{in}} \\ \mathrm{TM}_{\mathrm{in}} \end{bmatrix}. \quad (A.7)$$

In the following analysis we work out expressions for the coefficients of $[R]$ in terms of the properties of the magnetooptic film, which we assume to be optically isotropic.

In general the dielectric properties of a magnetooptic medium may be described by a *gyration vector* g which features in the equation relating D and E as

$$\boldsymbol{D} = \varepsilon\boldsymbol{E} + i\boldsymbol{E}\times\boldsymbol{g}. \quad (A.8)$$

For an isotropic medium the dependence of $\boldsymbol{g}$ on the external field is one of simple proportionality, and ε, too, reduces to a scalar n^2, where n is the refractive index. We define a right-hand set of coordinate axes x_i $(i = 1,2,3)$ with x_3 parallel to the waveguide propagation direction, x_2 also in the film plane, and x_1 directed normal to the film from substrate to top layer (Fig. 6 refers). The dielectric constant tensor referred to these axes is therefore given by

$$D_i = \sum_{j=1}^{3} K_{ij}^{x}E_j = n^2E_i + i\sum_{j=1}^{3}\sum_{k=1}^{3} e_{ijk}E_jg_k \quad (A.9)$$

where e_{ijk} is an antisymmetrical unit tensor.

If we assume that the magnetization is directed along the propagation direction x_3, then $g_1 = g_2 = 0$ and $g_3 = G$ (say). The dielectric tensor then takes on the special form

$$(K_{ij}^{x}) = \begin{bmatrix} n^2 & iG & 0 \\ -iG & n^2 & 0 \\ 0 & 0 & n^2 \end{bmatrix}. \quad (A.10)$$

It will be convenient to transform the problem to new axes (y_i) where y_3 is directed along the "zigzag" raypath in the film. If y_2 is set parallel to x_2 then the TE and TM electric fields will be directed along y_2 and y_1, respectively. The transformation matrix relating (x_i) and (y_i) is given by $y_i^{\pm} = a_{ij}^{\pm}x_j$, the $\pm$ superscript referring to "up" and "down" rays, respectively. If θ is the angle of incidence of "zigzag" wave (Fig. 6), then we write

$$(a_{ij}^{\pm}) = \begin{bmatrix} \cos(\pi/2 - \theta) & 0 & \mp\sin(\pi/2 - \theta) \\ 0 & 1 & 0 \\ \pm\sin(\pi/2 - \theta) & 0 & \cos(\pi/2 - \theta) \end{bmatrix}. \quad (A.11)$$

We can now refer the dielectric tensor of the magnetic film to the axes (y_i) and find that

$$(K_{ij}^{y})^{\pm} = a_{ik}^{\pm}a_{jl}^{\pm}(K_{kl}^{x}) = \begin{bmatrix} n^2 & iG\sin\theta & 0 \\ -iG\sin\theta & n^2 & \mp iG\cos\theta \\ 0 & \pm iG\cos\theta & n^2 \end{bmatrix}. \quad (A.12)$$

If we assume an $\exp[i(\omega t - \boldsymbol{kr})]$ dependence of the fields the electromagnetic wave equation reduces to

$$k^2\boldsymbol{E} - \boldsymbol{k}(\boldsymbol{k}\cdot\boldsymbol{E}) = k_0^2\boldsymbol{K}^{y}\cdot\boldsymbol{E}. \quad (A.13)$$

Let as assume a solution of the form $\exp[i(\omega t - \gamma k_0 z)]$ where, for ease of indexing, we replace y_3 by z, y_2 by y, and y_1 by x. We therefore obtain from (A.13) that

$$\gamma^2(\boldsymbol{i}E_x + \boldsymbol{j}E_y) = \begin{bmatrix} n^2 & iG\sin\theta \\ -iG\sin\theta & n^2 \end{bmatrix}\begin{bmatrix} \boldsymbol{i} & E_x \\ \boldsymbol{j} & E_y \end{bmatrix} \quad (A.14)$$

and hence

$$\gamma^2 = (n^2 \pm G\sin\theta) \quad \text{and} \quad E_x = \pm iE_y. \quad (A.15)$$

Equation (A.15) shows us the well known result that the eigenmodes of propagation are circularly polarized with propagation constants

$$\gamma^{r,l} = (n^2 \pm G\sin\theta)^{1/2}. \quad (A.16)$$

Notice that the *same* result is obtained for both the "up" and the "down" rays. In order to work out the mode conversion that takes place in one transit (up or down) of the zigzag path we decompose each of the TE and TM polarizations into two counter rotating circularly polarized modes. We let these propagate along the ray path length $W/\cos\theta$ and then reform the TE and TM polarizations.

Thus

$$E_x(z) = \frac{E_x(0)}{2}\exp(-ik_0\gamma_z{}^r) + \frac{E_x(0)}{2}\exp(-ik_0\gamma^l z) + i\frac{E_y(0)}{2}\exp(-ik_0\gamma^r z) - i\frac{E_y(0)}{2}\exp(-ik_0\gamma^l z) \tag{A.17}$$

$$E_y(z) = -i\frac{E_x(0)}{2}\exp(-ik_0\gamma^r z) + i\frac{E_x(0)}{2}\exp(-ik_0\gamma^l z) + \frac{E_y(0)}{2}\exp(-ik_0\gamma^r z) + \frac{E_y(0)}{2}\exp(-ik_0\gamma^l z). \tag{A.18}$$

At $z = 0$ we find that $E_x(z = 0) = E_x(0)$, and $E_y(z = 0) = E_y(0)$. Equations (A.17) and (A.18) can be factorized by noting, for example, that

$$-ik_0\gamma^r z = -\frac{i}{2}(\gamma^r - \gamma^l)k_0 z - \frac{i}{2}(\gamma^r + \gamma^l)k_0 z.$$

Thus

$$E_x(z) = \exp\left(-\frac{ik_0(\gamma^r + \gamma^l)z}{2}\right)\left\{E_x(0)\cos\left[\frac{k_0(\gamma^r - \gamma^l)z}{2}\right] + E_y(0)\sin\left[\frac{k_0(\gamma^r - \gamma^l)z}{2}\right]\right\} \tag{A.19}$$

$$E_y(z) = \exp\left(-\frac{ik_0(\gamma^r + \gamma^l)z}{2}\right)\left\{E_x(0)\sin\left[\frac{k_0(\gamma^r - \gamma^l)z}{2}\right] + E_y(0)\cos\left[\frac{k_0(\gamma^r - \gamma^l)z}{2}\right]\right\}. \tag{A.24}$$

From (A.16) we find $(\gamma^r + \gamma^l)/2 = n$ and $(\gamma^r - \gamma^l)/2 = (G\sin\theta)/2n$ and, since we can identify TE modes with E_y and TM modes with E_x, we find that the matrix defined in (A.7) can be written from (A.19) and (A.20) as

$$[R_{\text{up}}] = [R_{\text{down}}] = \exp(i\Delta)\begin{bmatrix}\cos\psi & -\sin\psi\\ \sin\psi & \cos\psi\end{bmatrix} \tag{A.21}$$

where

$$\Delta = -\frac{k_0 nW}{\cos\theta} \quad \text{and} \quad \psi = -\frac{k_0 GW\tan\theta}{2n}.$$

This is the desired matrix.

ACKNOWLEDGMENT

The author wished to express his gratitude for the facilities provided by the U.S. Naval Research Laboratory. He also wishes to thank his colleagues T. G. Giallorenzi, W. K. Burns, and A. F. Milton for many stimulating discussions.

REFERENCES

[1] J. Helsazan, *Principles of Microwave Ferrite Engineering.* New York: Wiley-Interscience, 1969.
[2] J. Warner, "Faraday optical isolator/gyrator design in planar dielectric waveguide form (*Invited Paper*)," *IEEE Trans. Microwave Theory Tech. (1973 Symposium Issue)*, vol. MTT-21, pp. 769–775, Dec. 1973.
[3] S. Wang, M. Shah, and J. D. Crow, *J. Appl. Phys.*, vol. 43, pp. 1861–1875, Apr. 1972.
[4] H. Kogelnik, T. P. Sosnowski, and H. P. Weber, "A ray-optical analysis of thin-film polarization converters," *IEEE J. Quantum Electron.*, vol. QE-9, pp. 795–800, Aug. 1973.
[5] S. E. Miller, *Bell Syst. Tech. J.*, vol. 33, pp. 661–719, May 1954.
[6] *Landolt Bornstein Physical Tables* (New Series, Group III, vol. 4a). Berlin, Germany: Springer, 1970, p. 344.
[7] J. Warner, *Mater. Res. Bull.*, vol. 9, Apr. 1974.
[8] G. Nath and S. Haussuhl, *Appl. Phys. Lett.*, vol. 14, pp. 154–156, 1969.
[9] J. Warner, *Appl. Opt.*, vol. 13, May 1974.
[10] P. K. Tien *et al.*, *Appl. Phys. Lett.*, vol. 21, pp. 394–396, Oct. 1972.